Sustainable Futures 10 (2025) 100848

Contents lists available at ScienceDirect

Sustainable Futures

journal homepage: www.sciencedirect.com/journal/sustainable-futures

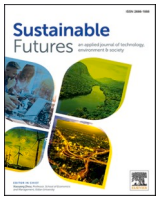

Enhancing frequency response using artificial intelligence techniques in the power system with renewable energy resources

M. Elzalik [a,*], Abouelmaaty M. Aly [b], Amir Y. Hassan [b], M.A. Abdelghany [c]

[a] Process Control Technology Department, Faculty of Technology and Education, Beni-Suef University, Egypt
[b] Power Electronics and Energy Conversion Department, Electronics Research Institute, Cairo, Egypt
[c] Electrical Engineering Department, Faculty of Engineering, October 6 University, Egypt

ARTICLE INFO

Keywords:
AI techniques
Load frequency control
PSO algorithm, Renewable energy generation (PV, and Wind)
Multi-generation
Low inertia

ABSTRACT

This article aims to improve the performance of the modern electric power system with renewable energy resources, which have fluctuating power and low inertia contribution, by designing a control system based on different artificial intelligent (AI) techniques. Because of this power fluctuation, there is a constant mismatch between generation and load, which causes the power system's frequency to vary. Low-inertia operation amplifies the frequency fluctuation at the same time. Due to the stochastic variation of load and renewable resources in the system, an effective load frequency control (LFC) technique is therefore required. When working conditions change, LFC based on a fixed controller may perform unsatisfactorily even though it may respond optimally at a specific operating point. With the constraints and nonlinearities of the system taken into account, the controllers are applied to the secondary loop LFC of a multi-source generating system. The power system's mathematical model was obtained using a transfer function approach, and the AI controllers were optimized using a particle swarm optimization technique (PSO) algorithm. Utilizing the FOPID reduces the settling time by 50.5 %, 64.6 % while FFOPID reduces it by 74.0 %, 81.4 % compared to optimal PID and FPID, respectively. Also, they reduces the system nadir for excessive load conditions. The results demonstrated that the power system's LFC is combined with AI controllers, the fuzzy fractional order proportional integral derivative (FFOPID) controller performs better than the other AI controllers.

1. Introduction

Renewable energy sources like photovoltaic (PV) and wind technologies have recently contributed significantly to the generation of electricity in electric power systems. Both the environment and the economy benefit from this generation scheme. Nevertheless, the electricity generated from renewable sources varies and cannot be dispatched [1]. Furthermore, there is a decrease in the contribution of system inertia. The frequency and voltage of the power system fluctuate as a result of this power fluctuation, which also continuously creates an inadvertent mismatch between generation and load. At the same time, the frequency deviation is suspected to be severe due to the reduction of the system inertia. High-frequency nadir and a high rate of frequency change are two ways that frequency fluctuation damages the load and generating equipment. Consequently, interference with the protection system could result in a cascading outage, generation trip, or load shading [2]. However, Egypt's electricity generation system is a multi-source system that includes hydroelectric, reheat, non-reheat, and renewable energy (including solar and wind) generating plants [3]. An effective load frequency control (LFC) technique is required due to the generating system's non-linearity and the stochastic variation of load and renewable resources.

Reducing transient frequency variations while maintaining zero steady-state inaccuracy is the main objective of LFC. According to the present study, a variety of approaches have been used in the LFC loops of different power systems [1,2]. There are three types of frequency support loops: primary frequency control, which is primarily carried out by the governor in conventional stations and acts within 30 seconds of a disturbance; secondary frequency control, which restores the frequency to the rated value by regulating the governor set point; and supplementary frequency support, which can be implemented using external energy storage systems like batteries, flywheels, super conductor magnet energy storage (SMES), etc. [4]. A better reaction is obtained when additional frequency support is utilized. By expanding the energy

* Corresponding author.
E-mail address: mohamed.abdelbar@techedu.bsu.edu.eg (M. Elzalik).

https://doi.org/10.1016/j.sftr.2025.100848
Received 31 December 2024; Received in revised form 13 April 2025; Accepted 11 June 2025
Available online 14 June 2025

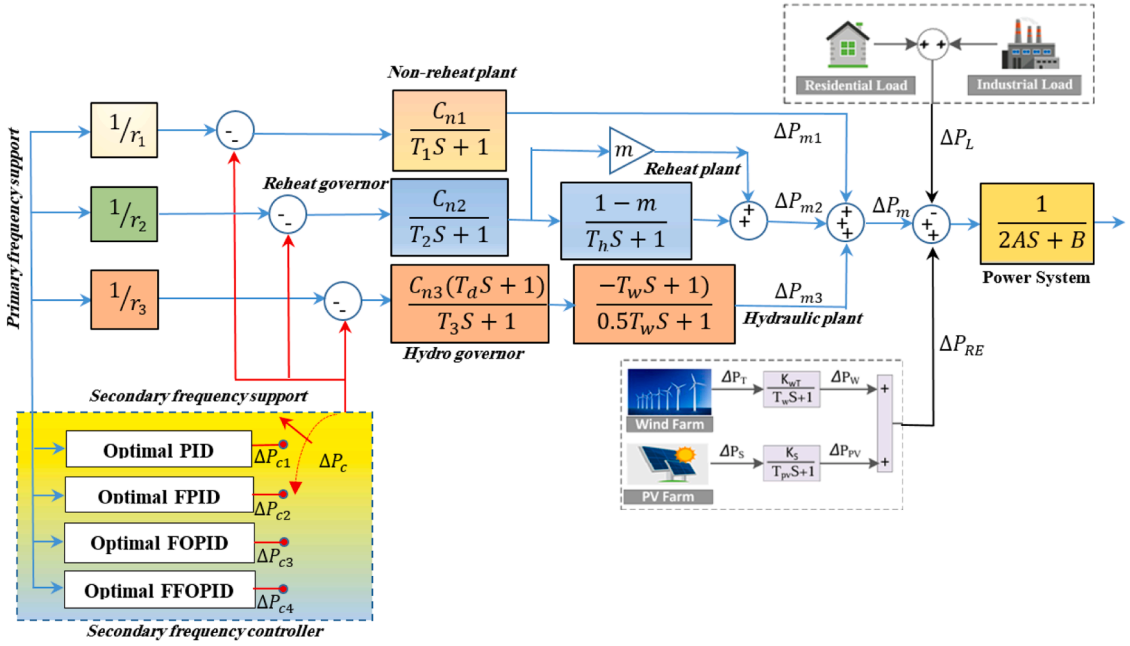

Fig. 1. Egyptian power system with LFC.

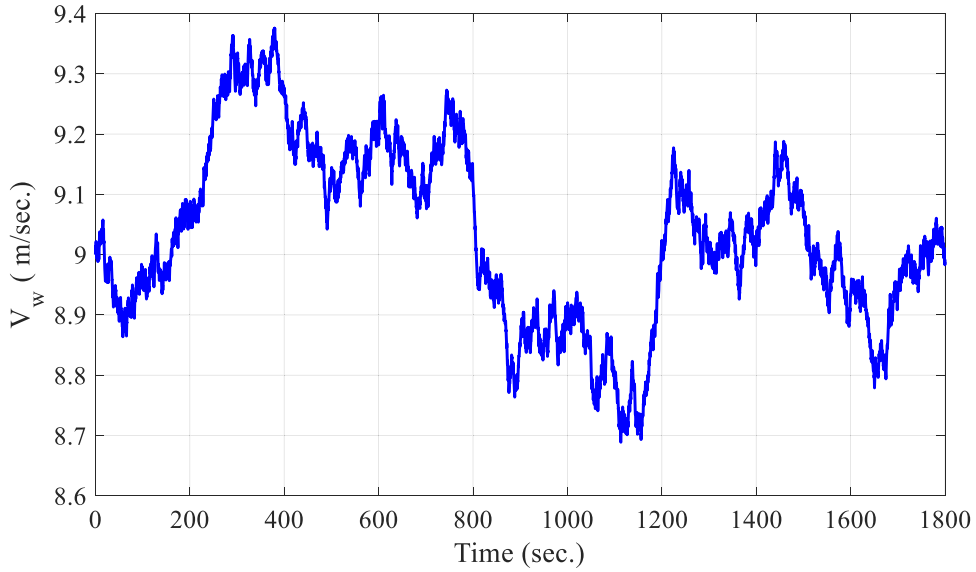

Fig. 2. Wind speed profile.

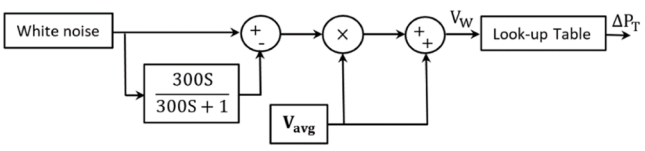

Fig. 3. Wind power generation pattern.

storage system's capacity, enhancement can be further enhanced. However, energy storage systems require an additional investment. Fuzzy fractional order proportional integral derivative (FFOPID) controller technique is used to improve secondary control loop performance.

The authors of [5] presented a strong LFC that uses the electric car as an energy storage component. In order to supply LFC in multi-source power systems, fractional-order PI and PD controllers have been proposed in [6]. For the LFC of three area power systems, two-degree of freedom PID (2-DOF-PID) has been used in [7]. The previously mentioned controllers are linear and can respond satisfactorily under design conditions, but because of the nonlinearity of the system, their reaction reduces when the operating point changes. A robust controller or nonlinear controller will be used for dealing with this nonlinearity. Fuzzy logic controllers are nonlinear controllers that can be used to counteract the nonlinearity of a system. They are characterized by their straightforward construction, ease of implementation, and potential applications. Fuzzy logic controllers can be implemented using a variety of techniques. The traditional Mamdani fuzzy controller is called fuzzy-PD [8], although fuzzy PI or fuzzy PID control can be used to remove the steady-state error [8–10]. In order to provide secondary frequency management in a multi-source system with SEMS and unified power flow, the authors in [11] have taken advantage of type II fuzzy

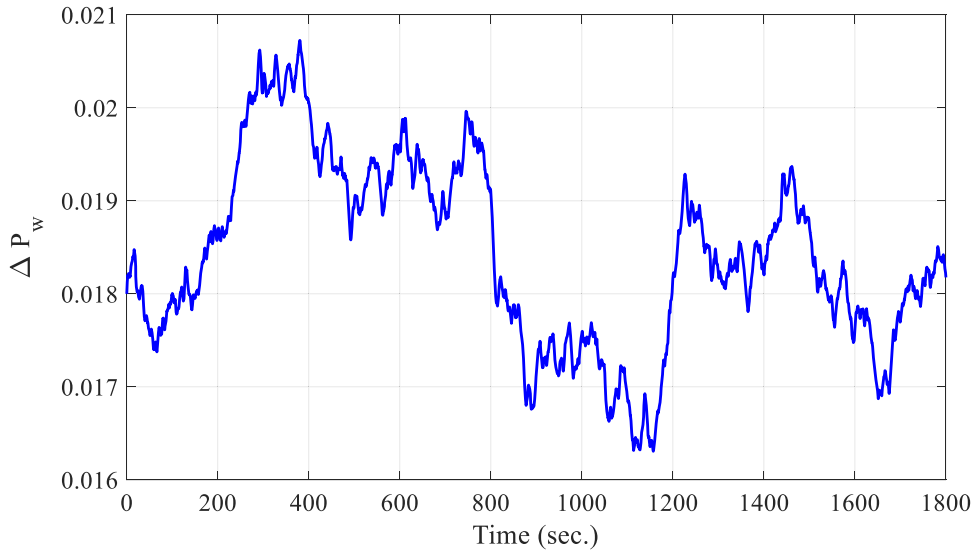

Fig. 4. Wind power profile.

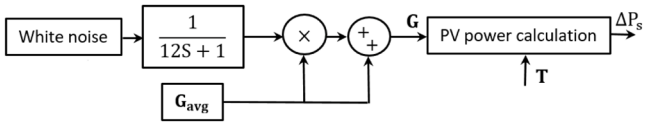

Fig. 5. Solar power generation patterns.

logic PID controller. In order to provide LFC service, a fuzzy self-tuned PD controller has been proposed in [12]. In [13], the controller parameters of traditional PID controllers were tuned online using a fuzzy. For LFC of two interconnected areas, fractional order fuzzy PID has been employed in [14].

For secondary frequency support in LFC, this research proposes a fuzzy fractional order proportional integral derivative (FFOPID). The tuning parameters of the suggested FFOPID must be carefully chosen while taking the nonlinearities of the system into account in order to properly exploit it. To optimize the controller parameters, a number of meta-heuristic optimization strategies have gained popularity recently. The magnetotactic bacteria optimization (MBO) approach, PSO, and GA were used in [5] to improve the robust LFC controller. The artificial sheep algorithm (ASA) was used in [8] to adjust the PI controller. Additionally, the Harris Hawks optimizer was used to optimize the PI controller in [15,16]. The dragonfly search algorithm (DSA) has been used to optimize the fractional-order PI and PD controllers to provide LFC in a multi-source power system [6]. By using a differential evolution algorithm (DE), the ideal fuzzy PID controller has been created to deliver LFC [9]. Fuzzy controllers, PD, PID, and self-tuning fuzzy PI have all been optimally designed using Artificial Bee Colony Optimization (ABCO) [13]. The fuzzy PID has been optimized by the authors in [11] using the water cycle algorithm (WCA). PSO is used in this article because of its robustness, ease of construction, and quick conversion. Also, the objective function takes into account the system restoration speed at disturbances, the frequency oscillation, and the frequency nadir. The focus of this study is primarily on the development and contribution of the objective function, which serves as the cornerstone of our methodology. The choice of the optimization technique, in this case, PSO, was made to demonstrate the efficiency of the proposed objective function. While it is true that other heuristic techniques such as GA, GWO, or HHO exhibit differences in convergence behavior, these

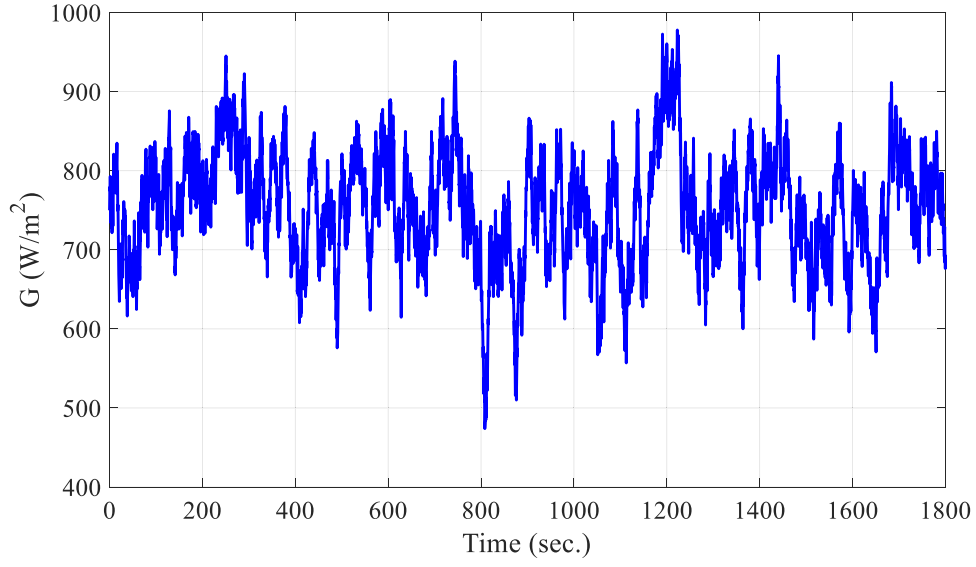

Fig. 6. Solar irradiance profiles.

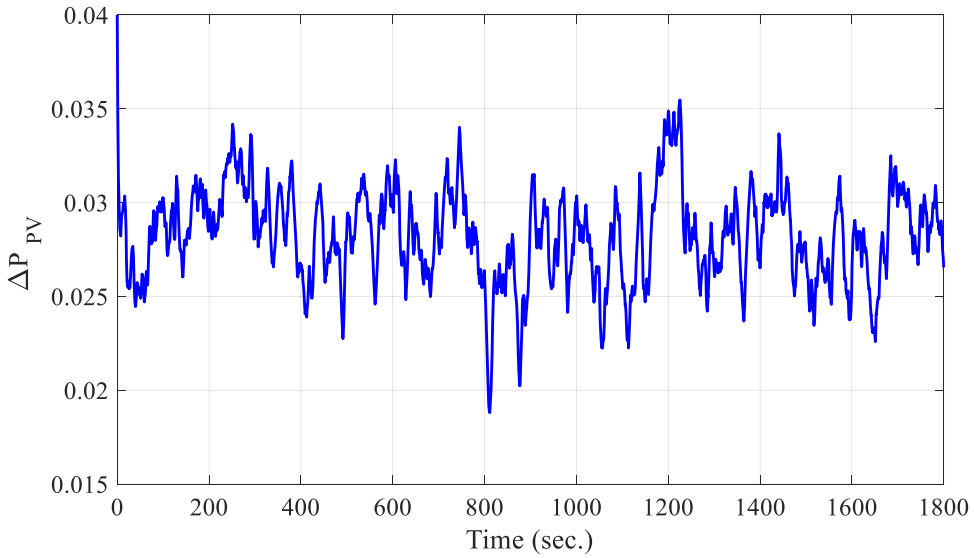

Fig. 7. PV power profile.

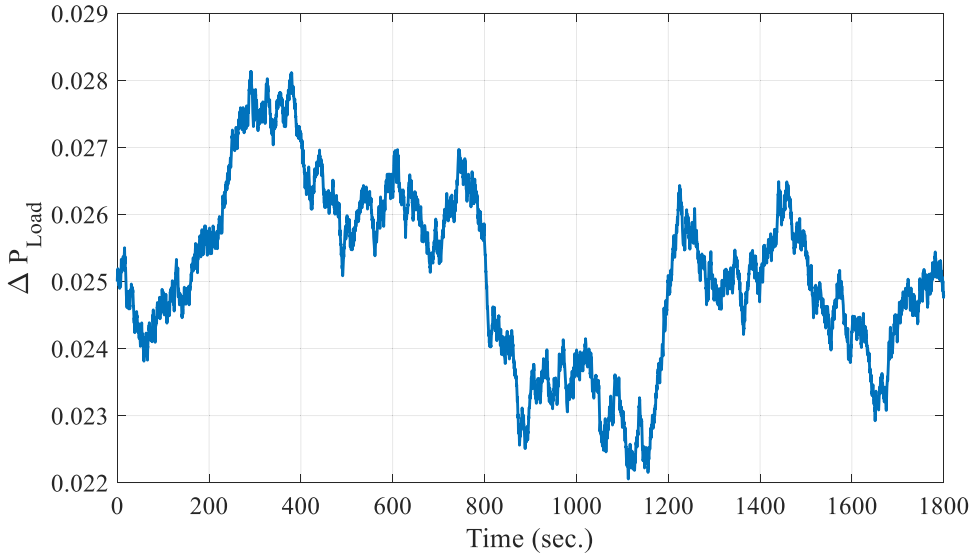

Fig. 8. Random load variation.

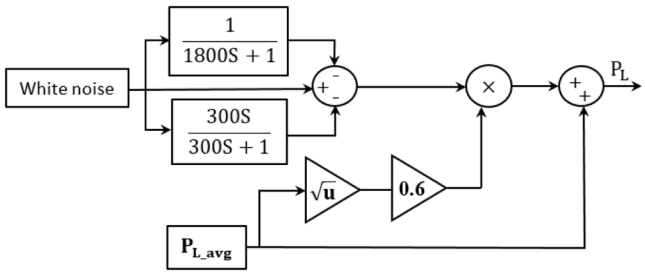

Fig. 9. Block diagram of fluctuated load profile generation.

differences are not central to the objectives of this study, as convergence time was not the primary concern. Our intention is to highlight the adaptability of the proposed objective function, which can be integrated with various optimization techniques if required in future work.

When designing a controller for real-world applications, it's critical to take the system's limitations and constraints into account in order to prevent damaging the system or its constituents and to improve the control system's performance. The Egyptian power system serves as a real-world case study for the suggested fuzzy fractional order proportional integral derivative (FFOPID) controller, see Fig. 1. The Egyptian power system load frequency control (EPSLFC) is used as a case study to test the suggested FFOPID controller. Step load power (SLP) change, random load variation, and various load characteristics, such as industrial and residential load, are among the simulations that are run. In addition, combining wind and solar power systems with inadvertent disconnections and reconnections. The controller is finally put to the test while the system's inertia is reduced. The result of system performance is compared with the other artificial intelligent (AI) controllers. The simulation's outcomes validate the recommended controller's superiority over alternative controllers.

The major contribution of this article is that the proposed FFOPID controller enhances the frequency response of a multi-generation system with renewable generation resources without using extra elements such as energy storage systems. Also, the optimizing the suggested controller and adaptation law gains through the use of a particle swarm optimization technique (PSO). Therefore, the nonlinearities of the system and

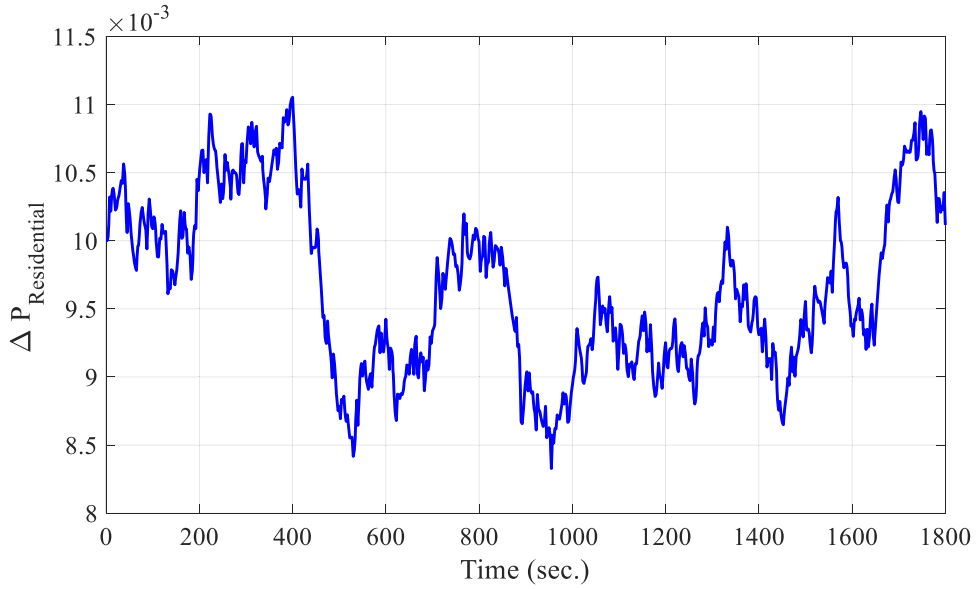

Fig. 10. Residential load random variation.

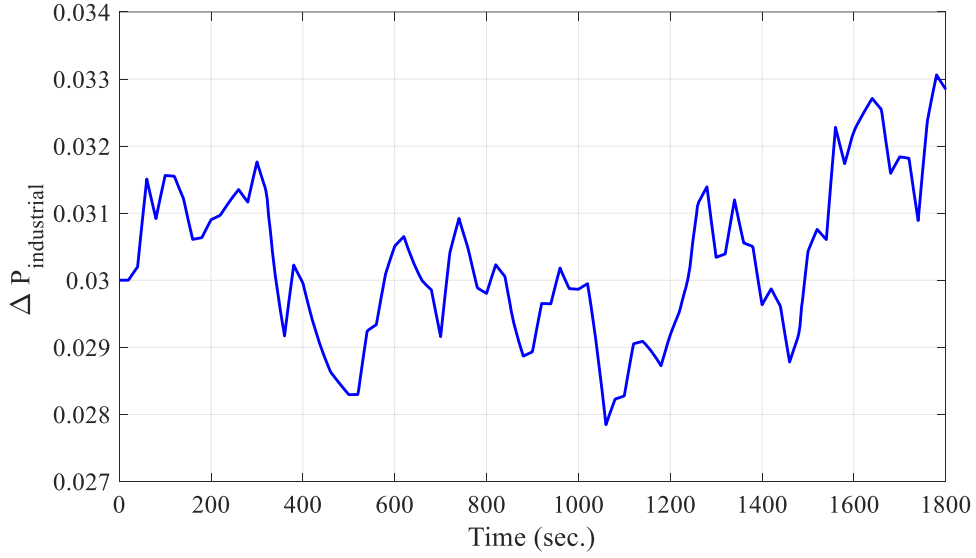

Fig. 11. Industrial load random variation.

the interactions between its components are incorporated into the design phase while reducing the effort required to design the controller using conventional techniques like Lyapunov methods. Furthermore, the response of the suggested controller is compared to that of the other AI controllers under various disturbances, including parameter variation, stochastic generation variation, and random load change.

The article's remaining sections are organized as follows: In section 2, the LFC power system model is shown in detail. Section 3 provides a detailed description of the tuning method and the suggested fuzzy fractional order proportional integral derivative (FFOPID) controller. The simulation results under various load and generation disturbances are shown and discussed in Section 4. Lastly, the results of the work that was presented are summed up in 5.

2. The modeling and description for the EPSLFC

As of the 2020 report, Egypt's power system has approximately a total installed generation capacity of 0.059 TW, with a peak load of 0.032 TW [17]. This capacity is divided across various energy sources: 0.002 TW from the high dam at Aswan (hydraulic), 0.054 TW from thermal power stations, and 0.003 TW from renewable sources such as solar and wind [18]. The Egyptian National Energy Control Center (ENECC) treats the power system as a single-area system, integrating these different generation technologies [19]. The following section provides further details on the system's model [20].

2.1. System block diagram

In the following subsection, the transfer function for each component of the proposed power system is presented. Additionally, the overall system block diagram is displayed to provide a comprehensive view of how the various parts of the power system interact. Each part of the system is modeled to capture its dynamic behavior, and the block diagram illustrates the interconnections between these components, allowing for a clear understanding of the system's overall performance and response. Fig. 1 illustrates the block diagram of the power system

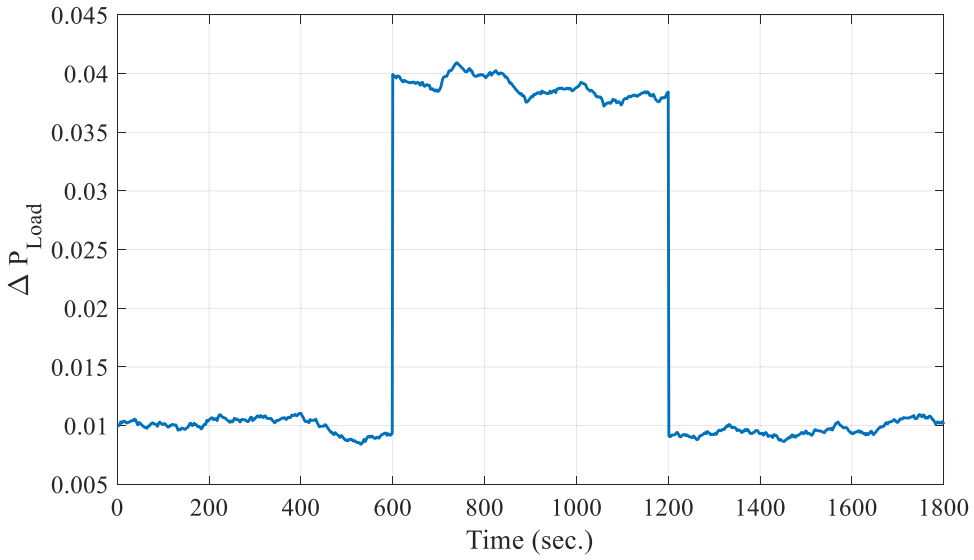

Fig. 12. Overall load variation.

Table 1
Egyptian power system parameters.

Non-reheat plant	
T_1	0.4 sec.
r_1	2.5 Hz/pu
C_{n1}	0.2529 p.u
Reheat plant	
T_2	0.4 sec.
T_h	6 sec.
r_2	2.5 Hz/p.u
C_{n2}	0.6107 p.u
m	0.5 p.u
hydraulic plant	
T_3	90 sec.
r_3	1.0 Hz/pu
C_{n3}	0.1364 p.u
T_d	5 sec.
T_w	1.0 sec.
Power System	
A	5.7096 sec.
B	0.028 p.u MW/Hz
Renewable plants	
T_{PV}	1.8 sec.
T_{WT}	1.5 sec.

applied different control techniques. The Generation Rate Constraints (GRC) are set at 10 % per minute for the reheat station, 20 % per minute for the second reheat station, and 50 % per minute for the hydraulic station.

2.1.1. Swing equation

The swing equation, which governs the frequency variation of the power system (PS), is represented by Eq. (1) [19]. In this equation, Δf denotes the frequency deviation, and ΔP_mrepresents the total mechanical power input to the grid from conventional generation units, including heat (ΔP_{m1}), reheat (ΔP_{m2}), and hydraulic stations (ΔP_{m3}). Additionally, ΔP_{RE} represents the total generated power from renewable resources, such as wind and PV systems, as illustrated in Eq. (2). The system's inertia constant is denoted by A, and the damping factor is represented by B. These parameters play key roles in the system's dynamic response to changes in power input and frequency variation.

$$\Delta f = \frac{1}{2As + B}(\Delta P_{m1} + \Delta P_{m2} + \Delta P_{m3} + \Delta P_{RE} - \Delta P_L) \tag{1}$$

$$\Delta P_{RE} = \Delta P_W + \Delta P_{PV} \tag{2}$$

2.1.2. Non-reheat station

The mechanical power of the reheat plant is expressed by Eq. (3), where ΔP_c represents the governor's set point, r_1 is the governor regulation factor, T_1 is the governor's time constant, P_{m1} is the per-unit nominal working capacity of the non-reheat plant, and C_{n1} refers to the nominal capacity of the non-reheat plant. This equation models the behavior of the reheat plant's mechanical power output, considering the governor's control settings and the dynamic response characteristics of the plant.

$$\Delta P_{m1} = \frac{C_{n1}}{T_1 s + 1}\left(-\frac{1}{r_1}\Delta f - \Delta P_c\right) \tag{3}$$

2.1.3. Reheat power station

The governor droop control for the reheat plant is represented by Eq. (4), where ΔP_c is the set point of the governor and ΔP_{g2} is the governor output of the reheat plant. The regulation factor for the reheat plant's governor is denoted as r_2, which governs the plant's response to frequency changes. To model the governor's dynamic response, which includes signal amplification and transformation, a first-order system is used, described by Eq. (5) [20]. In this system, T_2represents the governor time constant, and C_{n2} refers to the nominal capacity of the reheat plant. This first-order model reflects how the governor adjusts the power output of the reheat plant in response to changes in system conditions.

$$\Delta P_{g2} = -\frac{1}{r_2}\Delta f - \Delta P_c \tag{4}$$

$$\Delta P_{V2} = \frac{C_{n2}}{T_2 s + 1}\Delta P_{g2} \tag{5}$$

The reheat power plant consists of multiple stages, including a high-pressure stage, a re-heater, and intermediate and low-pressure stages. The high-pressure stage is represented as a fraction of the governor's output, denoted by m as given in Eq. (6). After the reheating process, the remaining power is modeled using a first-order system, with the re-heater's time constant, T_h, describing the dynamic behavior as given in Eq. (7) [20]. The total mechanical power output of the reheat power plant is then calculated by considering all these stages and processes is

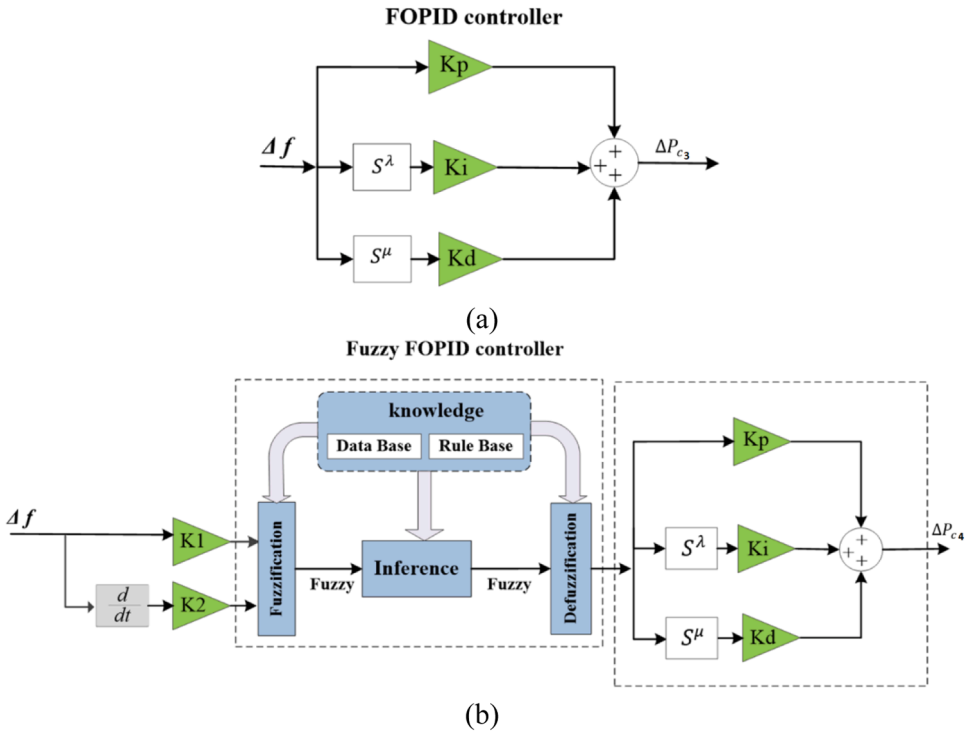

Fig. 13. (a) FOPID, and (b) Fuzzy FOPID control techniques.

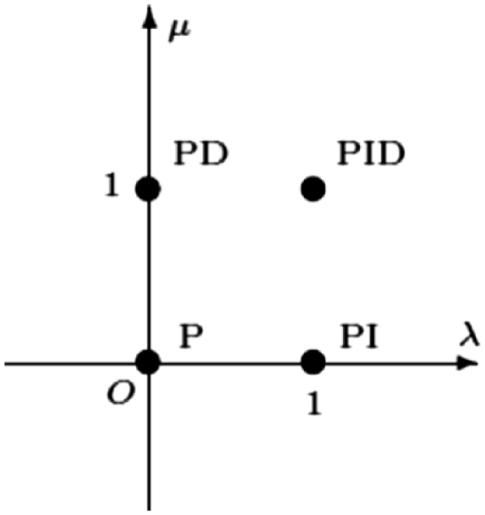

Fig. 14. PID/FOPID gains variation.

given by Eq. (8).

$$\Delta P_{m2\_hp} = m\Delta P_{V2} \tag{6}$$

$$\Delta P_{T\_lp\_Lp} = \frac{1-m}{T_h s+1}\Delta P_{V2} \tag{7}$$

$$\Delta P_{m2} = \Delta P_{m2\_hp} + \Delta P_{m2\_lp\_Lp} \tag{8}$$

2.1.4. Hydraulic power station

The governor droop control of the hydraulic station is described by Eq. (9), where ΔP_crepresents the governor's set point and ΔP_{g3} is the governor output of the hydraulic plant. The governor regulation factor for the hydraulic plant is denoted by r_3. The dynamics of the hydro governor, which include the dashpot time T_d, is modeled by Eq. (10). In this equation, C_{n3} is the nominal capacity of the hydraulic plant. The output power of the hydraulic station is determined using the turbine-penstock model, as shown in Eq. (11). This model incorporates the water time constant T_W, also known as the water starting time, and C_{n2}, which is the nominal capacity of the reheat plant [21].

$$\Delta P_{g3} = -\frac{1}{r_3}\Delta f - \Delta P_c \tag{9}$$

$$\Delta P_{V3} = C_{n3}\frac{T_d s+1}{T_3 s+1}\Delta P_{g3} \tag{10}$$

$$\Delta P_{m3} = \frac{-T_w s+1}{0.5T_W s+1}\Delta P_{V3} \tag{11}$$

2.1.5. Wind generation system model

The wind generation system captures wind energy and converts it into mechanical power using a wind turbine. The system typically operates at the maximum power point (MPP), but when wind speed fluctuates, the turbine adjusts its speed to stay at the MPP. This transition takes some time, which can be simplified and modeled using a first-order transfer function with a time constant T_{WT}. The output power of the wind turbine is represented by ΔP_{WT}. The available power from the turbine as shown in Eq. (12), ΔP_T, is determined by the turbine's characteristics, wind turbine control, and the wind speed [22].

$$\Delta P_{wT} = \frac{K_{WT}}{T_{WT} s+1}\Delta P_T \tag{12}$$

The wind speed is assumed to change randomly, as shown in Fig. 2. This signal is generated using MATLAB Simulink as shown in Fig. 3. The manufacturing data are stored in a look-up table, which is used during simulation to determine the output power of the wind turbine as shown in Fig. 4.

2.1.6. PV generation system model

The PV system converts solar energy into electricity using a PV array. The system's control mechanism regularly checks the PV array's

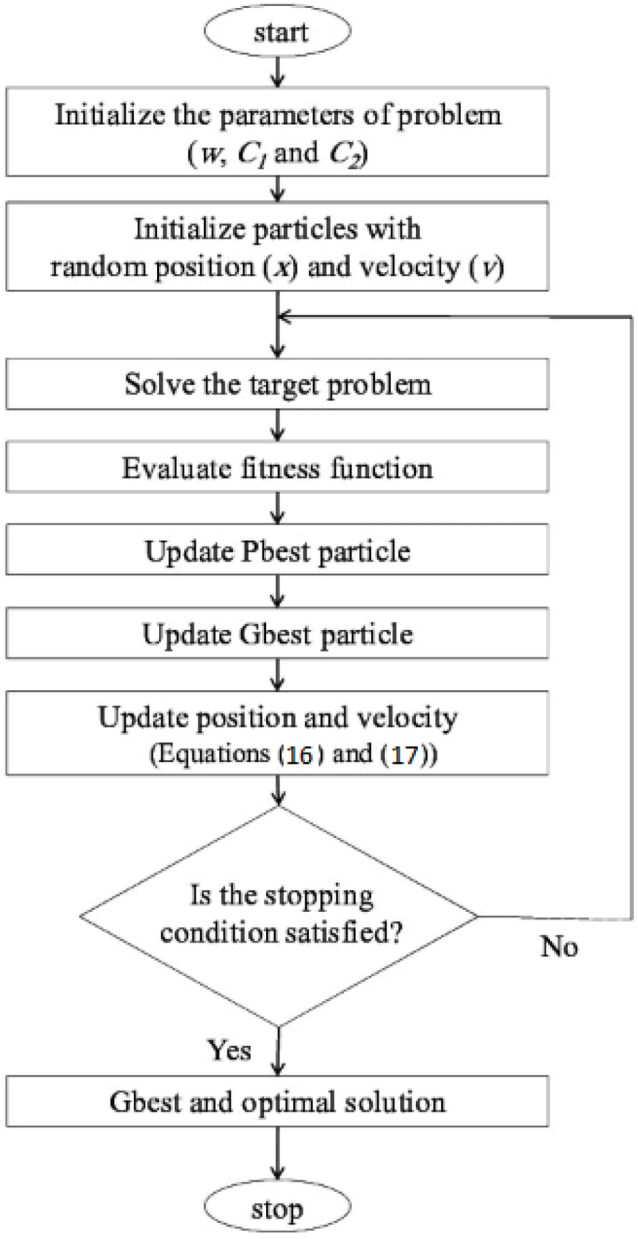

Fig. 15. Particle swarm optimization flowchart.

performance to ensure it operates at MPP. This process is modeled as a first-order system with a time constant T_{PV} as shown in Eq. (14). In this model, ΔP_s represents the amount of solar power converted, while ΔP_{PV} refers to the output power of the PV system.

$$\Delta P_{PV} = \frac{K_s}{T_{pv}s + 1}\Delta P_s \tag{14}$$

The generated power from the PV system depends on solar irradiance and temperature. For short-term simulation, the irradiance is assumed to vary randomly and the ambient temperature is fixed. The solar irradiance is generated using a white noise signal as shown in Figs. 5 and 6. The generated power from the solar array is given in Eq. (14) as shown in Fig. 7. Where: P_v , P_{STC} , G, α_{pv}, and T are the PV generated power, the rated power at STC, the solar irradiance, the temperature power coefficient, and module temperature; respectively.

2.1.7. Random variation of load model

Herein, to imitate the real load fluctuation, the load is assumed to vary randomly as shown in Fig. 8. This load profile is generated from a white noise with an average value of 0.025pu and variance of 0.6 as shown in Fig. 9. Electrical loads can be classified into residential and industrial loads, and each of them has different characteristics. The residential load is usually small compared to the industrial. It also has a higher fluctuation feature. In this work, the residential loads are assumed to vary as shown in Fig. 10, and the industrial is shown in Fig. 11. These load profiles are generated using a block diagram in Fig. 9 with different average and white noise frequencies. The system is assumed to be working on the residential load. After that, the industrial load is suddenly connected and disconnected again as shown in Fig. 12.

Further details and other parameters can be found in Table 1.

3. The proposed FOPID and FFOPID controllers

These controllers are used to regulate the frequency of the system. Fractional order PID (FOPID) control combined with fuzzy logic improves the system's performance. In FOPID control, a type of PID control, a fractional order calculator defines the proportional, integral, and derivative terms [24]. Fractional-order calculus allows designers more flexibility in tailoring the controller to specific system requirements. The PSO algorithm is used to adjust the optimum values of all controllers applied to the frequency control of a power system as a case study. The FOPID includes five parameters: Kp, Ki, Kd, μ, and λ as shown in Fig. 13 (a). The FFOPID controller comprises of fixed rule base fuzzy controller, which was used in [20], with the five parameters of FOPID as shown as Fig. 13(b).

3.1. Fractional-order PID (FOPID)

The greatest option for more effective fractional order control of a dynamic system is a fractional order PID controller. To give an additional degree of freedom through orders of the integral and derivative in addition to controller gains, a typical PID controller can be generalized as $PI^{\lambda}D^{\mu}$ [23] controller with an integrator of order λ and a differentiator of order μ. The following is an expression for a controller's transfer function of the FOPID controller [25]:

$$G_C(S) = K_p + \frac{K_i}{S^{\lambda}} + K_d S^{\mu} \tag{15}$$

The fractional-order derivative (μ) and the fractional-order integration (λ) are both positive real numbers. Fig. 14 shows how the parameter plane of the $PI^{\lambda}D^{\mu}$ controller can expand to the full λ-μ plane from that of the traditional PID controller respectively.

A dynamic system can be efficiently controlled thanks to this expansion's increased control design flexibility in tuning parameter

Table 2
Different controller's gains are optimized by PSO.

Controller Type	Optimization gains	Optimal gains							
		k_p	k_i	k_d	k_u	μ	λ	k_1	k_2
Optimal PID [20]	K_p, K_i and K_d	3.476	0.079	0.508	-	-	-	-	-
Optimal FPID [20]	K_p, K_i, K_d and K_u	0.245	29.832	0.802	0.392	-	-	-	-
Optimal FOPID	K_p, K_i, K_d, μ and λ	7.746	0.919	9.758	-	0.310	0.843	-	-
Optimal FFOPID	K_p, K_i, K_d, μ, λ, K_1 and K_2	5.760	5.710	3.809	-	0.195	0.303	3.724	10.842

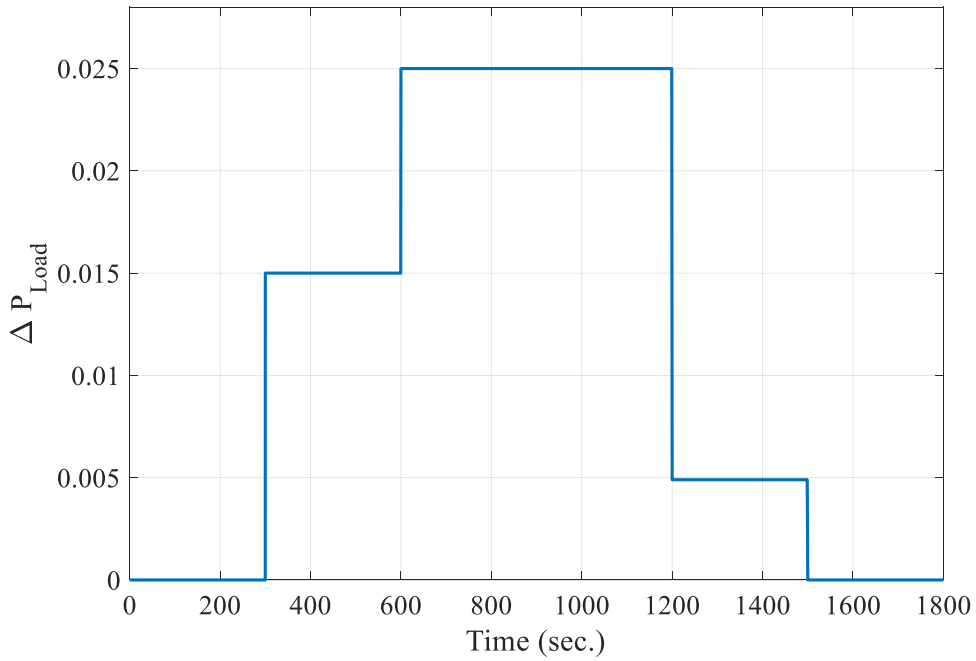

Fig. 16. Step load disturbance.

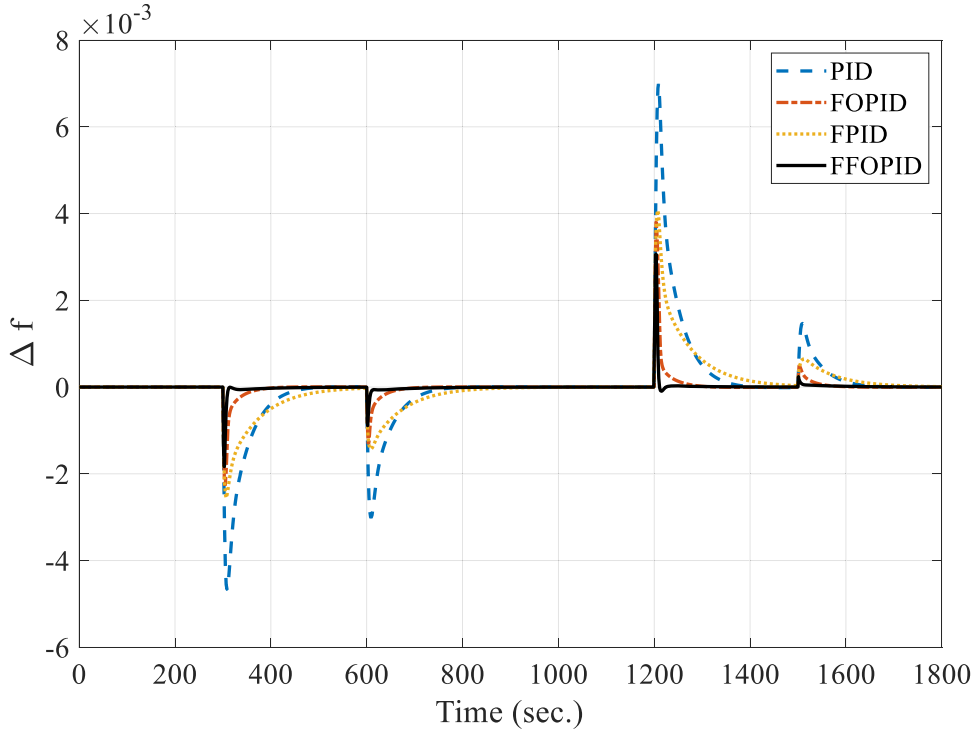

Fig. 17. Frequency response of the Egyptian Power System during a step load variation, indicating that the FFOPID Controller provides the best response.

Table 3
Performance indicators at step load change.

Controller Type	$\Delta P_L = 1.5\%$				$\Delta P_L = 2.5\%$			
	t_s (s)	Nadir (p.u)	Nadir (Hz)	ITAE (Hz.s^2)	t_s (s)	Nadir (p.u)	Nadir (Hz)	ITAE (Hz.s^2)
PID	210	0.0047	0.2332	655.36	120	0.0030	0.1504	243.4
FPID	255	0.0026	0.1278	284.25	289	0.0014	0.0714	783.2
FOPID	160	0.0023	0.1135	36.52	87	0.0013	0.0654	124.4
FFOPID	100	0.0018	0.0917	5.41	59	0.0008	0.0439	95.6

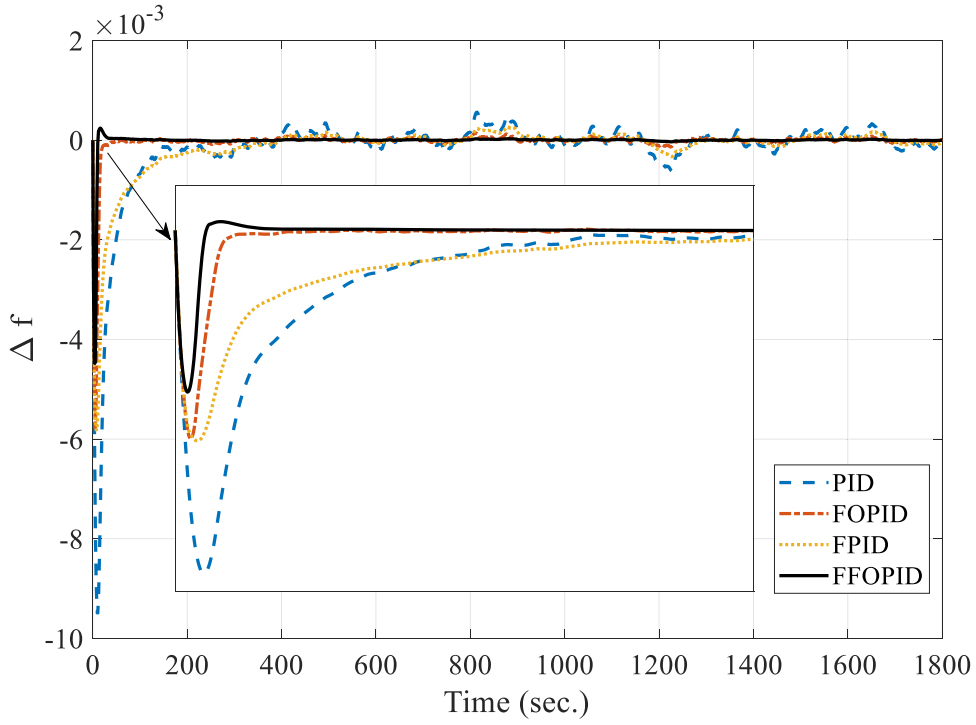

Fig. 18. Frequency response of the EPS under random load variation, FFOPID controller delivers the most effective response.

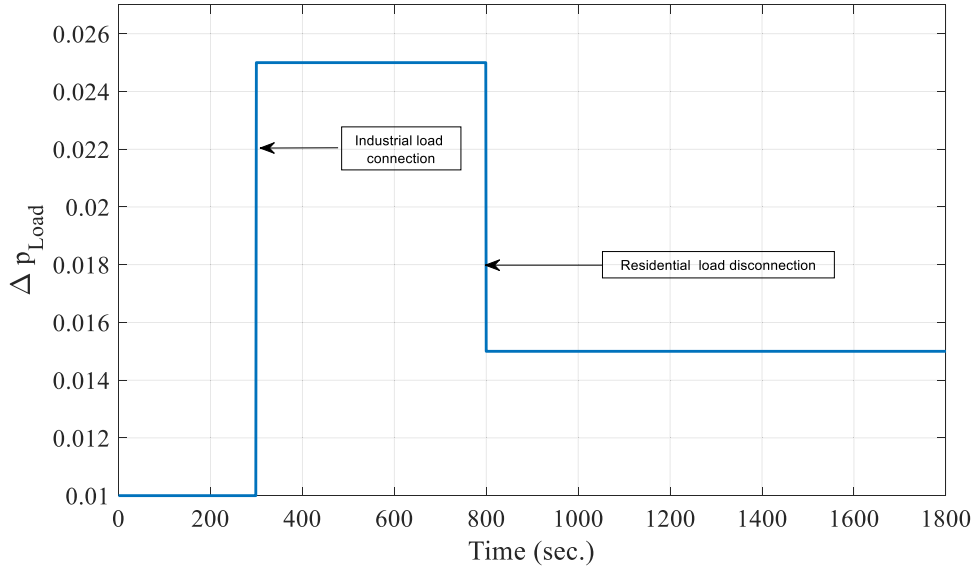

Fig. 19. Residential and industrial load.

selection. Additionally, the system performance is improved by the $PI^{\lambda}D^{\mu}$ controller's decreased sensitivity to changes in the controlled system's characteristics.

In this work, PSO algorithm is used to optimize the values of fractional-order derivative and integration (μ, λ). The PSO algorithm is featured by fast computation time, simple construction, and fast conversion among many available optimization techniques such as Bat Algorithm, Bee Colony Optimization (BCO), Grasshopper Optimization (GO), Artificial Bee Colony (ABC), Ant Colony Optimization (ACO), Firefly (FF) optimization, Cuckoo Search Optimization (CSO), Grey Wolf Optimization (GWO), etc. The PSO imitates the behavior of a swarm, where each solution represents a particle in the swarm. The particle updates its position according to its experience represented by the personal best position and social interaction imitated by the global best of swam. The calculation of the new position involves only two equations. Eq. (16), is the updated velocity of the particle, and Eq. (17) is the updated position of the particle i. Where: v_i^n, v_i^{n+1} are the particle current and updated velocities. The G_{best}, $P_{best,i}$ are the global and the particle best position; w, C_1, C_2 are the inertia, social, and personal factors; b_1, b_2 are random numbers [0 1]; and x_i^n, x_i^{n+1} the current and updated particle position. The particles and population are evaluated according to the predefined fitness function, the flowchart of PSO is represented in Fig. 15. The applied fitness function is given in Eq. (18). The first term represents the integral absolute error (ITAE), since minimization of the ITAE makes the system fast response. The second term minimizes the oscillation of the system frequency, and the last term

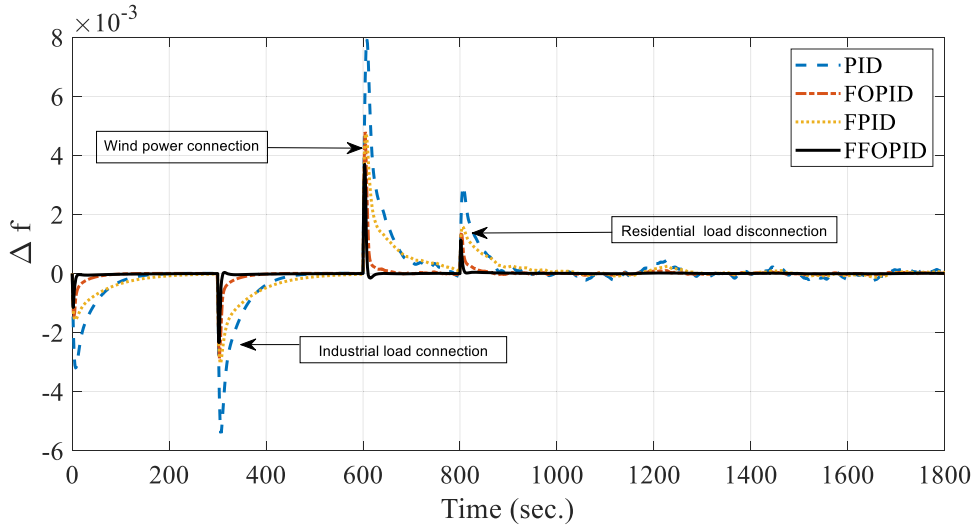

Fig. 20. Frequency response of the Egyptian Power System with wind integration, FFOPID controller yields the optimal response.

Table 4
Performance indicators connection and disconnection of residential and industrial load.

Controller Type	Connection of industrial load (2.5 %)			Disconnection of residential load (1.5 %)		
	t_s (s)	Nadir (p.u)	Nadir (Hz)	t_s (s)	Nadir (p.u)	Nadir (Hz)
PID	200	0.0054	0.2702	97	0.0030	0.1478
FPID	280	0.0031	0.1524	231	0.0016	0.0790
FOPID	99	0.0029	0.1445	59	0.0014	0.0704
FFOPID	52	0.0023	0.1162	20	0.0011	0.0564

minimizes the system rate of change of frequency (ROCOF). The objective function gains O_1, O_2, and O_3 are weighting gains and unit conversion. In order to limit the frequency nadir and ROCOF with fast response, the nadir, ROCOF, and ITAE shall be considered concurrently in the optimization problem. The resultant multi-objective function is given by Eq. (18), which is commonly referred by weighted-sum approach. In the weighted-sum approach, all terms are summed after multiplication by weighting factor to convert multi-objective function into a single objective function. The weighting factors play two roles. The first role is scaling, since the term with the higher weight is relatively more important. The second role is to make all scaled terms have the same unit of measurement. To achieve the second role, the unit of each weighting factor is assumed based on the required objective function unit and the unit of the corresponding pre-scaled term. From the simulation results in the next sections, multi-objective function succeeds to provide less frequency nadir and better ROCOF. The optimization problem is subjected to constraints given by inequalities for Eq. (19). The optimal controller's gains are given in Table 2.

$$v_i^{n+1} = w v_i^n + C_1 b_1 \left(P_{best,i} - x_i^n\right) + C_2 b_2 \left(G_{best} - x_i^n\right) \tag{16}$$

$$x_i^{n+1} = x_i^n + v_i^{n+1} \tag{17}$$

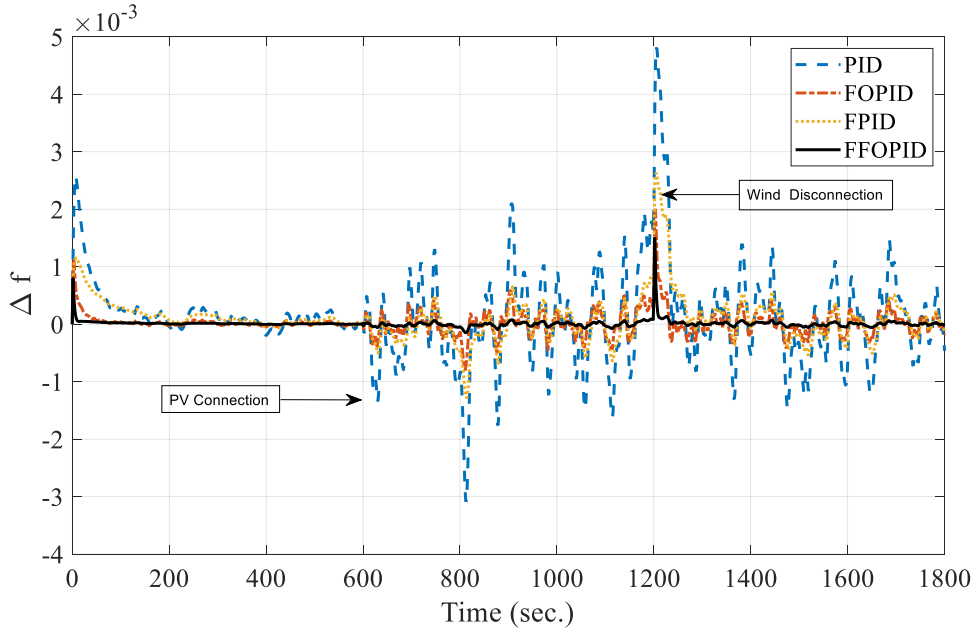

Fig. 21. Frequency response of the EPS system with renewable energy resources and variations in industrial and residential loads, FFOPID controller achieves the best results.

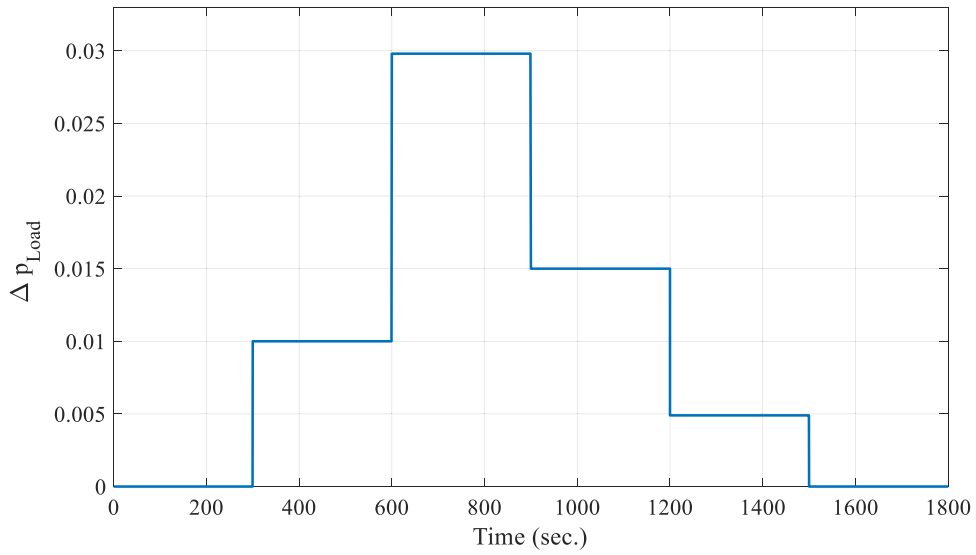

Fig. 22. Step load disturbance.

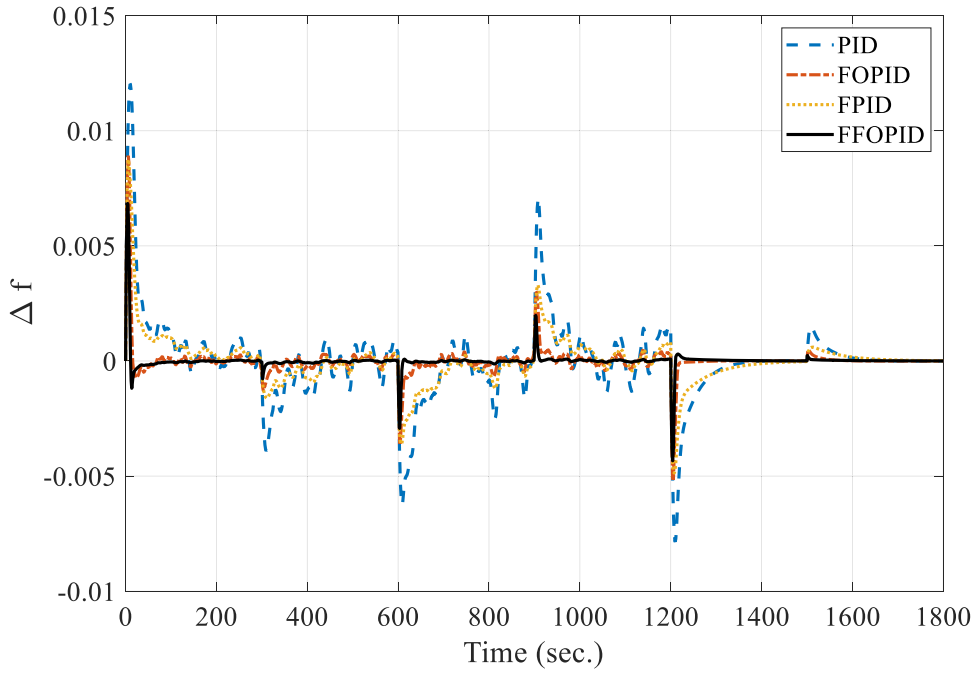

Fig. 23. Illustrates the frequency response of the Egyptian Power System during step load variation with the PV disconnected, FFOPID controller provides the optimal response.

$$OF = \min\left[O_1 \int_0^t t\lceil \Delta f \rceil dt + O_2 \max(\Delta f, 0) + O_3 \frac{\Delta f}{\Delta t}\right] \tag{18}$$

Subject to:

$$k_p^{min} \le k_p \le k_p^{max}$$

$$k_d^{min} \le k_d \le k_d^{max}$$

$$k_i^{min} \le k_i \le k_i^{max}$$

$$k_u^{min} \le k_u \le k_u^{max}$$

$$\mu^{min} \le \mu \le \mu^{max}$$

$$\lambda^{min} \le \lambda \le \lambda^{max}$$

$$k_1 min \le k_1 \le {k_1}^{max}$$

$$k_2 min \le k_2 \le {k_2}^{max} \tag{19}$$

4. Results of the simulation

The performance of the power system under investigation is examined using various load frequency controllers while various disturbances are present, such as step and random load variation, fluctuations in renewable generation, generation outages, and inertia reduction.

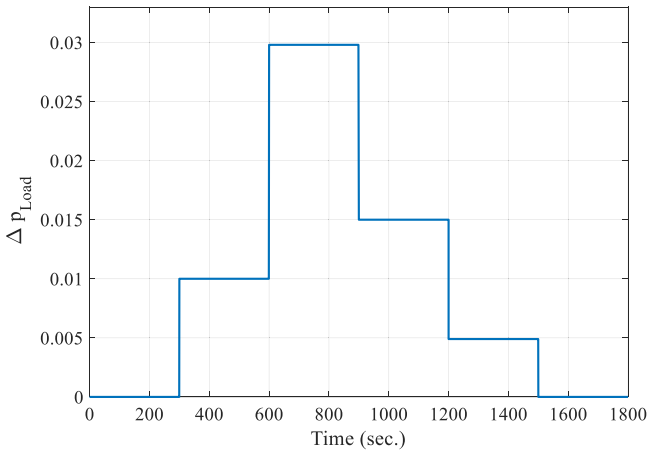

Fig. 24. Step load variation.

4.1. Case 1: The load is changing in steps

In this case, the load is changing in steps as shown in Fig. 16. The frequency response under PID, FPID, FOPID, and FFOPID is shown in Fig. 17. From the results, the Fuzzy PID controller succeeded to reduce under/over frequency at load increase/decrease compared to the conventional PID. However, it takes a longer time. On the other hand, the two proposed controllers (FOPID and FFOPID) succeeded to reduce the over/under frequency and the setting time simultaneously. Also, when compare the new controllers, it is clear that the FFOPID is the more accurate than FOPID for over/undershot and the setting time. At 1.5 % load increase disturbance (at 300sec), the settling time is 210sec, 255sec,160sec and 100sec using PID, FPID, and the two proposed controllers (FOPID and FFOPID) respectively. While at 2.5 % load disturbance (at 600sec), the settling time becomes 120sec, 289sec, 87sec, and 59sec using PID, FPID, FOPID and FFOPID controllers respectively. Hence, the two proposed controllers provide a faster response compared to the other controllers and FFOPID is the best. Moreover, at 1.5 % load disturbance, the frequency nadir is0.2332Hz, 0.1278Hz, 0.1135Hz, and 0.0917Hz with the PID, the FPID, and the two proposed FOPID, FFOPID controllers respectively. Also, at 2.5 % load disturbance, the frequency nadir becomes0.1504Hz, 0.0714Hz, 0.0654Hz, and 0.0439Hz with PID, FPID, FOPID and FFOPID controllers respectively. Therefore, the two proposed controllers produce a significant reduction in the system nadir among other controllers. Eventually, the two proposed controllers provide less Integral Time Absolute Error (ITAE) compared to the other applied controllers as indicated in Table 3.

4.2. Case 2: random variation of load for EPS without renewable energy

According to the random variation of load as shown in Fig. 8, the PID and FPID controllers maintain the system stability while the fluctuation in frequency is higher among other controllers as shown in Fig. 18. The two proposed controllers (FOPID and FFOPID), keep the system frequency at the desired value with less oscillation and fast response; note that the response of FFOPID controller is better than the FOPID controller.

4.3. Case3: Residential and industrial load with Wind connected

Industrial load disturbance abruptly increases by 2.5 % at 300 seconds, while residential load is disconnected by 1.5 % at 800 seconds, as shown in Fig. 19. The wind power generation is connected at 600 seconds. Fig. 20 shows, both suggested controllers (FOPID and FFOPID), keep the system frequency at the desired value with less oscillation and fast response; note that the response of FFOPID controller is better than the other controllers (i.e., FOPID, FPID and PID controllers). The summary of the comparison between the different controllers is given in Table 4.

4.4. Case 4: Random variation of load for EPS with renewable energy resources

According to the scenario of the random variation of load model in subsection 2.1.7, the frequency response is shown in Fig. 21. It is obvious that when the industrial load is connected at the same time with the solar power generation (i.e. 600sec.), the system frequency decreases, and when the industrial load is disconnected at the same time with the wind power generation (i.e. 1200sec.), the frequency increases. The two

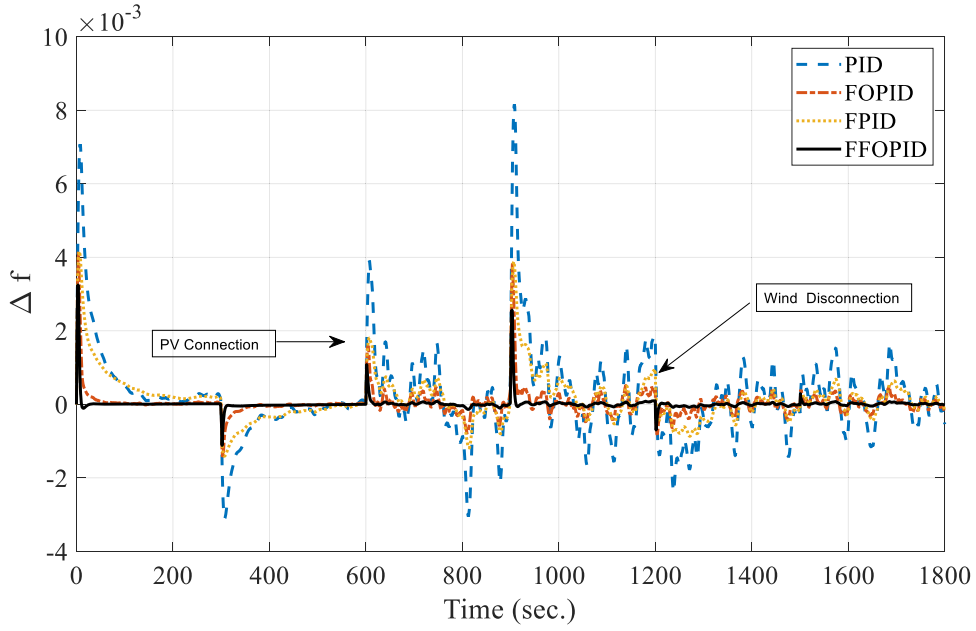

Fig. 25. Frequency response with a 25 % reduction in inertia, FFOPID controller provides the optimal response and demonstrates better than other control performance.

proposed controllers restore the system frequency with less frequency deviation and less settling time. Also, during industrial load connection, the system with PID and FPID controllers has higher oscillation compared to residential load operation due to larger load fluctuation. On the other hand, the proposed controllers successfully limit the effect of this larger load fluctuation. Therefore, even with wider load power fluctuation, the proposed controllers introduce a superior response compared to PID and FPID.

4.5. Case 5: The load is changing in steps with PV disconnected

Here, the controller's performance is investigated with solar power, and the load varies in stages, as seen in Fig. 22. Here, the solar power generation is disconnected at 1200 seconds. As seen in Fig. 23, the two recommended controllers (FOPID and FFOPID) maintain the system frequency at the intended level with reduced oscillation and quick reaction; it should be noted that the FFOPID controller responds more quickly than the FOPID, FPID, and PID controllers.

4.6. Case 6: Operation at inertia reduction by 25 % at step load variation

In this case, the controller performance is investigated in the presence of solar, wind generation, and the load is changing in steps as shown as Fig. 24. However, the system inertia is reduced by25 %. Fig. 25 shows that reduction of the system inertia causes higher frequency deviation since, at solar power connection at 600sec while wind power is disconnected at 1200sec. As a result, a decrease in system inertia increases the frequency deviation, which could cause the protection relay to activate. The suggested controllers outperform the optimal PID, and optimal FPID in terms of frequency deviation, oscillation, and settling time.

5. Conclusion

This work proposed two AI controllers which are unlike the classical controllers since these controllers, FOPID and FFOPID, have an online adjustable rule base. The controllers are applied to provide a secondary LFC service in the Egyptian power system as a practical multi-source generation. At step load change by 1.5 %, the setting time is 160sec and 100sec using FOPID and FFOPID, respectively. The system obtained an ITAE of 36.52Hz.s^2, 5.41Hz.s^2 and the frequency nadir of 0.1135Hz and 0.0917Hz with the FOPID and FFOPID, respectively. Therefore, at step change in load, the proposed controllers provided a significant reduction in the frequency nadir, faster settling time and lower ITAE compared to the optimal classical PID and fuzzy PID controllers. Also, for excessive load conditions such as a large industrial load connection (2.5 % disturbance), the proposed controllers (i.e. FOPID and FFOPID) reduce the system nadir by 46.52 %, 57.00 % and 5.18 %, 23.75 % compared to optimal PID and FPID, respectively. The proposed controllers obtained less settling time by 50.5 %, 64.6 % for FOPID and 74.0 %, 81.4 % for FFOPID comparing to optimal PID and FPID, respectively. For reduce load conditions such as a small residential load connection (1.5 % disturbance), the proposed controllers (i.e. FOPID and FFOPID) reduce the system nadir by 52.37 %, 61.84 % and 10.89 %, 28.61 % compared to optimal PID and FPID, respectively. In addition, for random variation in load and fluctuation in the generated power from renewable resources (PV and wind), the proposed controllers succeeded to damp the system fast and providing a non-oscillating response among the other controllers. When disconnecting the PV generation, the two recommended controllers (FOPID and FFOPID) maintain the system frequency at the intended level with reduced oscillation and quick reaction.

CRediT authorship contribution statement

M. Elzalik: Writing – review & editing, Writing – original draft, Visualization, Validation, Supervision, Software, Resources, Project administration, Methodology, Investigation, Funding acquisition, Formal analysis, Data curation, Conceptualization. **Abouelmaaty M. Aly:** Writing – review & editing, Writing – original draft, Visualization, Validation, Supervision, Software, Resources, Project administration, Methodology, Investigation, Funding acquisition, Formal analysis, Data curation, Conceptualization. **Amir Y. Hassan:** Writing – review & editing, Writing – original draft, Visualization, Validation, Supervision, Software, Resources, Project administration, Methodology, Investigation, Funding acquisition, Formal analysis, Data curation, Conceptualization. **M.A. Abdelghany:** Validation, Software, Resources, Project administration, Methodology.

Declaration of competing interest

The paper demonstrates [This research work aims to improve the performance of the modern electric power system with renewable energy resources, which have fluctuating power and low inertia contribution, by designing a control system based on different artificial intelligent (AI) techniques. Because of this power fluctuation, there is a constant mismatch between generation and load, which causes the power system's frequency to vary. Low-inertia operation amplifies the frequency fluctuation at the same time. Due to the stochastic variation of load and renewable resources in the system, an effective load frequency control (LFC) technique is therefore required. When working conditions change, LFC based on a fixed controller may perform unsatisfactorily even though it may respond optimally at a specific operating point. With the constraints and nonlinearities of the system taken into account, the controllers are applied to the secondary loop LFC of a multi-source generating system. The power system's mathematical model was obtained using a transfer function approach, and the AI controllers were optimized using a particle swarm optimization technique (PSO) algorithm. The results demonstrated that the power system's LFC is combined with AI controllers, the fuzzy fractional order proportional integral derivative (FFOPID) controller performs better than the other AI controllers.].

Data availability

Data will be made available on request.

References

[1] Mohamed.A. Abdelghany, Fathy A. Syam, Abouelmaaty M. Aly, Mohamed. A. Abido, Shorouk Ossama Ibrahim, Load frequency and virtual inertia control for power system using fuzzy self-tuned PID controller with high penetration of renewable energy, J. Electr. Syst. Inf. Technol. 50 (11 November 2024) 1–16, https://doi.org/10.1186/s43067-024-00173-x.
[2] Magdi A. Mosa, Mariem Y. Yousef, Said M.El Masry, A.M. Abdel Ghany, A.A. Ali, Frequency support of AC microgrid with high penetration of photovoltaic using super-capacitor, Sustain. Energy Technol. Assess. 53 (2022) 102364.
[3] Ibrahim A. Nassar, Kholoud Hossam, Mahmoud Mohamed Abdella, Economic and environmental benefits of increasing the renewable energy sources in the power system, Energy Rep. 5 (2019) 1082–1088.
[4] Mahmoud M. Mohamed, Helmy M.El Zoghby, Soliman M. Sharaf, Magdi A. Mosa, Optimal virtual synchronous generator control of battery/supercapacitor hybrid energy storage system for frequency response enhancement of photovoltaic/diesel microgrid, J. Energy Storage 51 (2022) 104317.
[5] Musa Khan, Haishun Sun, Yingmeng Xiang, Di Shi, Electric vehicles participation in load frequency control based on mixed H2/H∞, Int. J. Electr. Power Energy Syst. 125 (2021) 106420.
[6] Emre. Çelik, Design of new fractional order PI–fractional order PD cascade controller through dragonfly search algorithm for advanced load frequency control of power systems, Soft Comput. 25 (2) (2021) 1193–1217.
[7] Neelesh Kumar Gupta, Manoj Kumar Kar, Arun Kumar Singh, Design of a 2-DOF-PID controller using an improved sine–cosine algorithm for load frequency control of a three-area system with nonlinearities, Prot. Control Mod. Power Syst. 7 (1) (2022) 1–18.
[8] Meysam Gheisarnejad, Mohammad Hassan Khooban, Secondary load frequency control for multi-microgrids: HiL real-time simulation, Soft Comput. 23 (14) (2019) 5785–5798.
[9] Neda Jalali, Hadi Razmi, Hasan Doagou-Mojarrad, Optimized fuzzy self-tuning PID controller design based on Tribe-DE optimization algorithm and rule weight

adjustment method for load frequency control of interconnected multi-area power systems, Appl. Soft Comput. 93 (2020) 106424.
[10] Mokhtar Shouran, Fatih Anayi, Michael Packianather, Monier Habil, Load frequency control based on the bees algorithm for the great britain power system, Designs 5 (3) (2021) 50.
[11] Ch Naga Sai Kalyan, B. Srikanth Goud, Ch Rami Reddy, Haitham S. Ramadan, Mohit Bajaj, Ziad M. Ali, Water cycle algorithm optimized type II fuzzy controller for load frequency control of a multi-area, multi-fuel system with communication time delays, Energies 14 (17) (2021) 5387.
[12] M.Reyasudin Basir Khan, Jagadeesh Pasupuleti, Razali Jidin, Load frequency control for mini-hydropower system: A new approach based on self-tuning fuzzy proportional-derivative scheme, Sustain. Energy Technol. Assess. 30 (2018) 253–262.
[13] Neelamsetti Kirn Kumar, Rahul Sanmugam Gopi, Ramya Kuppusamy, Srete Nikolovski, Yuvaraja Teekaraman, Indragandhi Vairavasundaram, Siripireddy Venkateswarulu, Fuzzy logic-based load frequency control in an island hybrid power system model using artificial bee colony optimization, Energies 15 (6) (2022) 2199.
[14] Anil Annamraju, Srikanth Nandiraju, Robust frequency control in a renewable penetrated power system: an adaptive fractional order-fuzzy approach, Prot. Control Mod. Power Syst. 4 (1) (2019) 1–15.
[15] Dalia Yousri, Thaniaknti Sudhakar Babu, Ahmed Fathy, Recent methodology based Harris Hawks optimizer for designing load frequency control incorporated in multi-interconnected renewable energy plants, Sustain. Energy Grids Netw. 22 (2020) 100352.
[16] Mohamed. Barakat, Novel chaos game optimization tuned-fractional-order PID fractional-order PI controller for load–frequency control of interconnected power systems, Prot. Control Mod. Power Syst. 7 (1) (2022) 1–20.
[17] New and Renewable energy authority, "Annual report 2020". http://nrea.gov.eg/Content/reports/Annual%20Report%202020%20En.pdf.
[18] M.A. Ghany, Mohamed A. Shamseldin, Parallel distribution compensation PID based on Takagi-Sugeno fuzzy model applied on Egyptian load frequency control, Int. J. Electr. Comput. Eng. 10 (5) (2020) 5274.
[19] Mariem Y. Yousef, Magdi A. Mosa, A.A. Ali, A.M.Abdel Ghany, M.A.Abdel Ghany, Load frequency control for power system considering parameters variation using parallel distributed compensator based on Takagi-Sugino fuzzy, Electr. Power Syst. Res. 220 (2023).
[20] M.A. Abdel Ghany, Magdi A. Mosa, A.M. Abdel Ghany, Mariem Y. Yousef, Improving the frequency response of a multi-generation power system using adaptive variable structure fuzzy controller, Electr. Power Syst. Res. 232 (2024) 110368.
[21] Abdullah Altay, Cem Şahin, Ires Iskender, Doğan Gezer, Caner Çakır, A compensator design for the aged hydroelectric power plant speed governors, Electr. Power Syst. Res. 133 (2016) 257–268.
[22] Li, Xiangjun, Dong Hui, Xiaokang Lai, and Tao Yan, "Power quality control in wind/fuel cell/battery/hydrogen electrolyzer hybrid micro-grid power system", IntechOpen, 2011.
[23] I. Podlubny, systems fractional-order and $PI^{\lambda}D^{\mu}$ controllers, IEEE Trans Autom. Control 44 (I) (1999) 208–214.
[24] M.N. Muftah, A. Athif, M. Faudzi, S. Sahlan, M. Shouran, Modeling and fuzzy FOPID controller tuned by PSO for pneumatic positioning system, Energies 15 (2022) 3757.
[25] I. Podlubny, Fractional-order systems and PI_D_ controllers, IEEE Trans. Autom. Contr. 44 (1999) 208–214.